J. Plasma Physics (2006), *vol.* 72, *part* 6, *pp.* 1025–1029.
doi:10.1017/S0022377806005150 Printed in the United Kingdom

Iterative numerical method for the inclusion of radiation trapping into a collisional–radiative model

KEIJI SAWADA

Faculty of Engineering, Shinshu University, 4-17-1, Wakasato, Nagano 380-8553, Japan

(Received 12 August 2005 and accepted 27 December 2005)

Abstract. The effect of radiation trapping is included in the standard collisional-radiative model for atomic hydrogen under a typical condition of divertor plasmas. The population of the first excited level of the ionizing plasma component is strongly enhanced by the absorption of resonance line photons produced by the recombining plasma component, and the effective ionization rate coefficient is also strongly enhanced.

1. Introduction

In divertor plasmas, radiation trapping is sometimes quite substantial: in the Alcator C-Mod divertor plasmas under detached conditions, for instance, it is found that up to 50% of the L_β emission is absorbed within the plasma [1], indicating that the L_α line is even more strongly absorbed than the L_β line. In applying the standard collisional-radiative model to such plasmas, we must properly include the effect of radiation trapping.

In the following we present our iterative method, which effectively solves the radiation transport equation.

2. Iterative numerical method

Our approach is based on the following algorithm. (1) Divide space into cubic cells of linear dimension Δl. (2) Give the ground state atom density $n(1)$, the ion density n_{H^+}, the electron density n_{e}, the electron temperature T_{e}, and the line profile function $g_{pq}(\nu)$ for the transition from upper level p to lower level q for each cell. Set the frequency interval $\Delta\nu$ for the following calculation of emission and absorption. (3) Compute the population distribution of excited levels for each cell using the ordinal optically thin collisional-radiative model [2] assuming no radiation trapping. (4) Compute the emission intensity radiated in each cell and the absorption in other cells using the population distributions obtained in step (3). (5) Compute the population distributions for each cell using the collisional-radiative model considering the absorption of photons. (6) Compute the emission intensity radiated in each cell and the absorption in other cells using the population distributions obtained in step (5). (7) Repeat steps (5) and (6). This iterative process is continued until the above values converge. The details are given in the following.

Optically thin collisional-radiative model

The collisional-radiative model has been used to calculate population distributions of the excited levels and the excitation and de-excitation flows between the levels [2]. The population of an excited level is given by the rate equation in which excitation, de-excitation and ionization by electron impact, three-body and radiative recombination, and spontaneous transition are included. In this paper, for simplicity, we neglect the contribution from molecules. In our code, the excited levels are specified by the principal quantum number and are considered up to 40. According to the quasi-steady-state solution [2], the population of the excited level p is given by

$$n(p) = R_0(p) n_{\mathrm{H}^+} n_{\mathrm{e}} + R_1(p) n(1) n_{\mathrm{e}} \quad (p \geqslant 2), \tag{2.1}$$

where $R_0(p)$ and $R_1(p)$ are functions of electron density and temperature. The first term and the second term are called the ionizing plasma component and the recombining plasma component, respectively [2]. The time development of the population of the ground state $n(1)$ is given by

$$\frac{dn(1)}{dt} = -S_{\mathrm{CR}} n(1) n_{\mathrm{e}} + \alpha_{\mathrm{CR}} n_{\mathrm{H}^+} n_{\mathrm{e}}, \tag{2.2}$$

where S_{CR} and α_{CR} are called the effective ionization rate coefficient and the effective recombination rate coefficient, respectively.

In our code, the atomic data are the same as in [2].

Inclusion of radiation trapping

The line profile function $g_{pq}(\nu)$ is defined so that the probability of emission in the interval $\nu \sim \nu + d\nu$ is $g_{pq}(\nu) d\nu$; the power radiated by any cell per unit frequency interval is given by $\varepsilon_{pq}(\nu) = A(p,q) n(p) g_{pq}(\nu) h\nu \Delta V$, where ΔV is the volume of the cell ($=\Delta l^3$). The radiated photons spread and may be absorbed by other atoms. Assuming isotropic photon emission, the energy density per unit frequency $\rho_{pq}(\nu)$ at a cell is calculated by

$$\rho_{pq}(\nu) = \frac{\varepsilon_{pq}(\nu)}{c} \frac{1}{4\pi r^2} \exp\left[-\int_0^r \kappa_{qp}(\nu)\, dl\right], \tag{2.3}$$

where r is the distance from the source to the cell, and c is the light velocity. The integration in exponential is on the line of sight from the source and the cell. Here, $\kappa_{qp}(\nu)$ is the absorption coefficient,

$$\kappa_{qp}(\nu) = \frac{[B(q,p) n(q) - B(p,q) n(p)] h\nu g_{pq}(\nu)}{c}, \tag{2.4}$$

where $B(q,p)$ and $B(p,q)$ is the Einstein B coefficient. We assume complete frequency redistribution: the same $g_{pq}(\nu)$ is used for absorption. By adding the contributions of photons coming from all of the cells, we calculate the total energy density per unit frequency $\rho_{pq}^{\mathrm{total}}(\nu)$ at each cell. We calculate the population of the excited atoms using the collisional-radiative model by adding the following term to the rate equation for $n(p)$:

$$\sum_{q \neq p} \left\{ [B(q,p) n(q) - B(p,q) n(p)] \sum_{\nu} \left[\rho_{pq}^{\mathrm{total}}(\nu) g_{pq}(\nu) \Delta\nu\right] \right\}.$$

https://doi.org/10.1017/S0022377806005150 Published online by Cambridge University Press

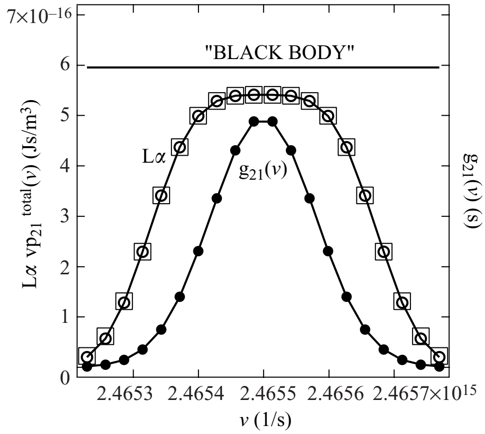

Figure 1. L_α spectrum at $z = 0$ m (○) and the line profile $g_{21}(\nu)$ (●). The 'BLACK BODY' line is calculated assuming a uniform infinite volume plasma whose population distribution is the same as that at $z = 0$ m. L_α spectrum calculated with $R_C = 8.0 \times 10^{-2}$ m for reference (□).

3. Results

We applied the above method to a plane-parallel slab which extends infinitely in the x and y directions, and from -5×10^{-3} to 5×10^{-3} m in the z-direction. It is assumed that the slab plasma has a uniform temperature $T_e = T_{H+} = T_H = 1$ eV, electron and proton density $n_e = n_{H+} = 10^{21}$ m^{-3}, and ground state density $n(1) = 10^{20}$ m^{-3}. The absorption of L_α and L_β are considered. It is assumed that the line profile function $g_{pq}(\nu)$ is given by the Doppler broadening. The value of $1/\kappa_{qp}(\nu)$ at the center frequency of L_α is 2.0×10^{-3} m; we divide the plasma volume into cubic cells of $\Delta l = 2.0 \times 10^{-4}$ m. We calculate the $\rho_{pq}^{\mathrm{total}}(\nu)$ along the z-axis considering the emission coming from cells within a cylinder with a radius of $R_C = 4.0 \times 10^{-2}$ m around the z-axis. For the integration in (2.3), the r-axis is divided into equal intervals of width $\Delta r = 2.0\times10^{-4}$ m. The ν-axis is also divided into equal intervals of width $\Delta\nu$ as shown in Fig. 1. Using $\rho_{pq}^{\mathrm{total}}(\nu)$ along the z-axis, the population density is calculated for each cell on the the z-axis. This population density is common to all the cells having the same z position in step (5).

Figure 2 shows the population of the excited levels calculated without the radiation trapping. Figures 3(a) and (b) show the dominant flux into and from each excited level for the recombining and the ionizing plasma components. The effective ionization and recombination rate coefficients without radiation trapping are $S_{CR} = 2.5 \times 10^{-19}$ and $\alpha_{CR} = 4.6 \times 10^{-18}$ (m^3 s^{-1}), respectively. Equation (2.2) is given numerically as

$$\frac{dn(1)}{dt} = -S_{CR}n(1)n_e + \alpha_{CR}n_{H+}n_e = -2.5 \times 10^{22} + 4.6 \times 10^{24}\,\mathrm{m}^{-3}\,\mathrm{s}^{-1}, \quad (3.1)$$

which means that the plasma is recombining.

The convergence requires about 10 iterations. The population distribution of the excited levels of the ionizing plasma component that are obtained after the convergence is achieved is shown in Fig. 2 (for the L_α line profile, see Fig. 1). In our framework, the recombining component is unaffected because the induced

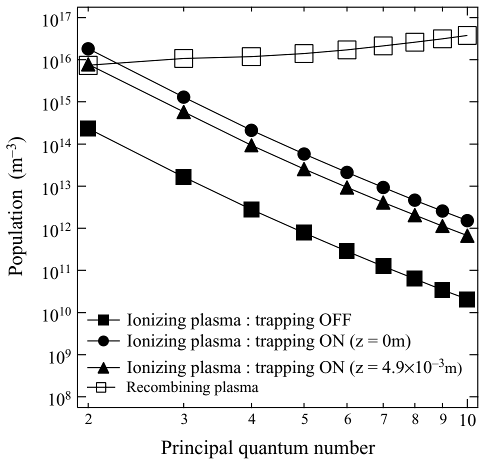

Figure 2. Population densities of the excited levels.

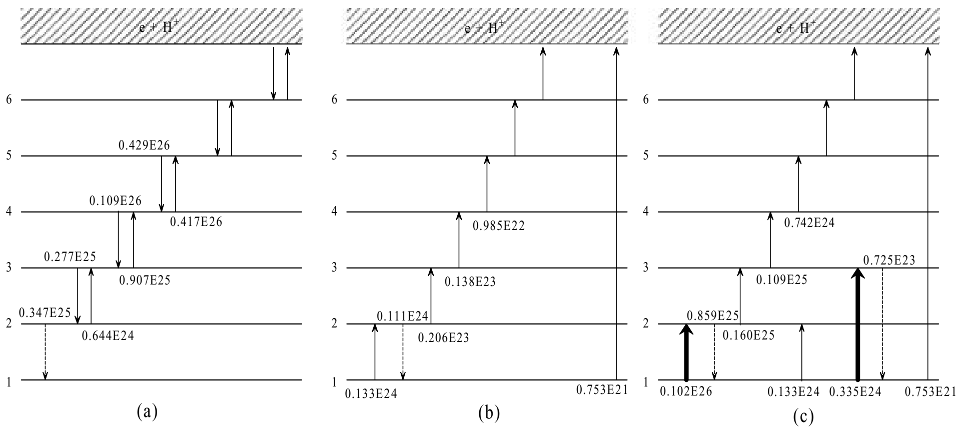

Figure 3. The excitation and de-excitation flow of (a) the recombining plasma component, (b) the ionizing plasma component (radiation trapping OFF), (c) the ionizing plasma component (radiation trapping ON) at the center $z = 0$ m of the slab. The figures of $1, 2, \ldots, 6$ denote the principal quantum number. The thin solid line, the broken line, and the thick solid line denote the transition by electron collision, the spontaneous emission, and the absorption of the photon, respectively. For example, 0.347E25 denotes 0.347×10^{25} m^{-3} s^{-1}.

emission is negligible. The population of the excited level $p = 2$ of the ionizing plasma component is enhanced to a value close to the recombining plasma component; Fig. 3(c) shows dominant flows among each excited level. The L_α photons emitted from the recombining component are absorbed by the ionizing plasma component. The population of the excited level $p = 2$ of the ionizing plasma component is established by the balance of the absorption of the photons which originate from the recombining component, and spontaneous emission. The effective ionization rate coefficient increases to $S_{CR} = 1.9 \times 10^{-17}$ m^3 s^{-1} due to the absorption of photons, which is followed by the ladder-like excitation–ionization for levels of $p \geqslant 2$. The

https://doi.org/10.1017/S0022377806005150 Published online by Cambridge University Press

α_{CR} does not change. Equation (2.2) is given numerically as

$$\frac{dn(1)}{dt} = -S_{\mathrm{CR}} n(1) n_{\mathrm{e}} + \alpha_{\mathrm{CR}} n_{\mathrm{H}^+} n_{\mathrm{e}} = -1.9 \times 10^{24} + 4.6 \times 10^{24}\,\mathrm{m}^{-3}\,\mathrm{s}^{-1}. \quad (3.2)$$

The plasma changed to an only slightly recombining plasma.

Acknowledgements

This study owes much to the thoughtful and helpful comments of Dr. T. Fujimoto. This research was supported by a Grant-in-Aid for Scientific Research (C) from the Ministry of Education, Science, Sports and Culture, and by the NIFS Collaborative Research Program.

References

[1] Terry, J. L., Lipschultz, B., Pigarov, A. Yu., Krasheninnikov, S. I., LaBombard, B., Lumma, D., Ohkawa, H., Pappas, D. and Umansky, M. 1998 Volume recombination and opacity in Alcator C-Mod divertor plasms. *Phys. Plasmas* **5**, 1759–1766.

[2] Fujimoto, T. 2004 In: *Plasma Spectroscopy*, Int. Series Monographs Phys, Vol. 123. Oxford: Oxford University Press.